

SCIENTIFIC REPORTS



OPEN

Distinct magnetic field dependence of Néel skyrmion sizes in ultrathin nanodots

F. Tejo¹, A. Riveros¹, J. Escrig^{1,2}, K. Y. Guslienko^{3,4} & O. Chubykalo-Fesenko⁵

We investigate the dependence of the Néel skyrmion size and stability on perpendicular magnetic field in ultrathin circular magnetic dots with out-of-plane anisotropy and interfacial Dzyaloshinskii-Moriya exchange interaction. Our results show the existence of two distinct dependencies of the skyrmion radius on the applied field and dot size. In the case of skyrmions stable at zero field, their radius strongly increases with the field applied parallel to the skyrmion core until skyrmion reaches the metastability region and this dependence slows down. More common metastable skyrmions demonstrate a weaker increase of their size as a function of the field until some critical field value at which these skyrmions drastically increase in size showing a hysteretic behavior with coexistence of small and large radius skyrmions and small energy barriers between them. The first case is also characterized by a strong dependence of the skyrmion radius on the dot diameter, while in the second case this dependence is very weak.

Magnetic skyrmions attracted recently enormous attention of researchers due to their promising static and dynamical properties resulting from their chiral magnetization configuration and non-trivial topology^{1–3}. The skyrmions possessing axial symmetry can be classified according to their internal structure. There are Bloch skyrmions (magnetization rotates in the plane perpendicular to the radial direction) and Néel or hedgehog skyrmions (magnetization rotates in the plane parallel to the radial direction, see Fig. 1). The former are typically stabilized by the relativistic Dzyaloshinskii-Moriya exchange interaction (DMI) in the bulk non-centrosymmetric crystals with B20 structure (like MnSi, FeGe, etc.) in the form of two-dimensional hexagonal lattices. Whereas, the Néel-type magnetic skyrmions can be stabilized as individual objects in ultrathin multilayer films, stripes and dots with DMI originating from the interfaces between transition metals (e.g. Co) and heavy metals with large spin-orbit coupling (Pt, Ir, Pd)^{4–7}. Although, the Néel skyrmion lattices were recently observed in the bulk polar crystals of GaV₄S₈⁸.

The interest of researchers to the individual Néel skyrmions is based on their promising technological perspectives because only individual nanoscale skyrmions can be used in any devices. First, several recent articles^{4,6,7} report that the isolated Néel skyrmions can be stable or metastable at room temperature opening the possibility for their use in information technology^{3,9}. Secondly, the magnetic skyrmions promise high thermal stability. This hypothesis comes from the idea of their topological protection, although no rigorous proof of the high thermal stability based on the energy barrier calculations exist^{10,11}. Furthermore, several studies also report on the possibility to move the Néel skyrmions by spin-polarised currents, especially with small current density values^{1,6,12} and to detect them by the spin-Hall effect^{13,14}. All these properties are extremely useful for future spintronic applications. These findings make skyrmions candidates for low energy consumption device applications and several designs for the skyrmions-based spin-torque nano oscillators, microwave detectors and logic devices were recently introduced^{3,9,15,16}.

The skyrmion stability and their equilibrium properties are important issues for any device applications. The skyrmion stability depends on all micromagnetic parameters, including the DMI, magnetic anisotropy strength, the exchange stiffness, and the applied magnetic field. Most of the works have been evaluating the stability diagram of individual skyrmions in dots as a function of the anisotropy and DMI strength^{17,18,19} (Aranda, A.R., *et al.*, Submitted,

¹Departamento de Física, Universidad de Santiago de Chile (USACH), Santiago, 9170124, Chile. ²Center for the Development of Nanoscience and Nanotechnology (CEDENNA), Santiago, 9170124, Chile. ³Departamento de Física de Materiales, Universidad del País Vasco, UPV/EHU, San Sebastián, 20018, Spain. ⁴IKERBASQUE, the Basque Foundation for Science, Bilbao, 48013, Spain. ⁵Instituto de Ciencias de Materiales de Madrid, Madrid, 28049, Spain. Correspondence and requests for materials should be addressed to O.C.-F. (email: oksana@icmm.csic.es)

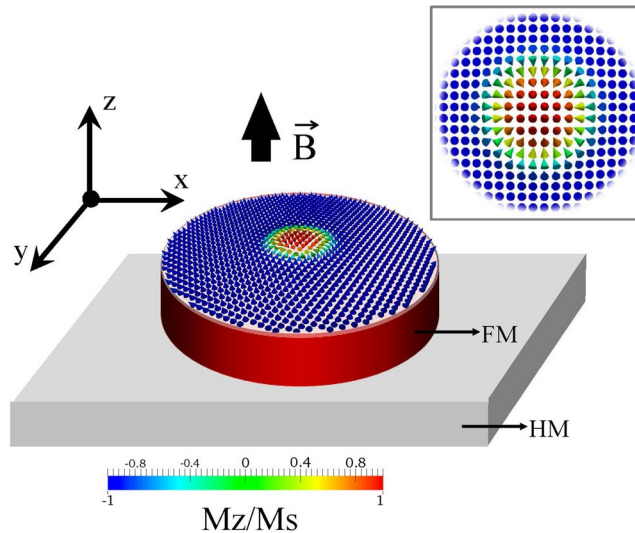


Figure 1. Ultrathin circular ferromagnetic (FM) nanodot on a heavy metal (HM) substrate. The Néel skyrmion magnetization profile is shown by the color map. The applied magnetic field (B) is in the z -direction and is perpendicular to the dot plane.

2018). On the other hand the stability of skyrmion lattices as a function of the applied magnetic field has been evaluated mostly in bulk magnets or infinite thin films see, e.g. refs^{20,21}. Rohart and Thiaville²² have suggested a simple formula coming from the cylindrical domain wall theory for the critical DMI strength D_c at which the skyrmion becomes energetically favorable, $D > D_c = (4/\pi)\sqrt{AK_{eff}}$, where A is the exchange stiffness parameter, $K_{eff} = K_u - \mu_0 M_s^2/2$ is the effective magnetic uniaxial anisotropy constant which includes perpendicular magnetocrystalline anisotropy constant K_u and the magnetostatic contribution, where M_s is the material saturation magnetization. In spite of the fact that this approach is not well justified^{17,23}, it gives a simple and frequently working estimation for the skyrmion stability edge in restricted geometry. Importantly, most of the Néel skyrmions are metastable states in absence of the applied magnetic field (Aranda, A.R., *et al.*, Submitted, 2018), i.e., have the magnetic energy larger than the perpendicularly magnetized states.

In many experimental works⁴⁻⁷ several skyrmions are uncontrollably present. For applications, however, individual skyrmions should be nucleated and manipulated. This can be done by geometrical confinement in patterned magnetic films (stripes, dots, etc.) with out-of-plane magnetic anisotropy. Recent calculations show that the skyrmion stability region is significantly modified due to the presence of magnetic sample boundaries¹⁹ and essential contribution of the magnetostatic energy. It has been demonstrated that the skyrmion stability depends on the dot size and the stability region is larger in dots with smaller sizes (Aranda, A.R., *et al.*, Submitted, 2018). For recent calculation of the stability diagram of Néel skyrmions in dots in terms of the perpendicular anisotropy and DMI strength see also¹⁸.

Following the approach of Rohart and Thiaville²², the radius of skyrmions has been predicted to reveal a strong increase as a function of the DMI parameter when approaching the critical value D_c for the metastability region. As a function of the applied magnetic field, the skyrmion radius (when the skyrmion core magnetization direction is antiparallel to that of the field) decreases as reported experimentally in ref.⁴ and increases when the core direction is parallel to the field direction, see also ref.²⁴.

In this article we systematically investigate the dependence of the Néel skyrmion radius on applied out-of-plane magnetic field in ultrathin circular magnetic dots with different sets of the micromagnetic parameters and dot sizes. We found a very distinct behavior of the skyrmion radius depending on the fact whether the skyrmion configuration is stable at zero field or metastable.

Model

To study the dependence of the skyrmion diameter and its stability in a ultrathin circular magnetic dot varying an out-of-plane external magnetic field we apply the micromagnetic approach. The geometry of physical system under study is depicted in Fig. 1, where we indicate that in our convention the positive out-of-plane magnetic field is parallel to the skyrmion core, while the negative field is applied anti-parallel to it. The dot has variable diameter d and fixed thickness of 0.6 nm. We consider different materials with the parameters taken from the literature and corresponding to different CoPt-based multilayer systems which we schematically indicate as PtCoPt¹², PtCoMgO⁷, IrCoPt⁴ and PtCoNiCo²⁵.

The system energy functional is defined by the following energy density

$$\varepsilon(\vec{m}) = A \sum_{\alpha=x,y,z} (\vec{\nabla} m_\alpha)^2 + D[m_z \vec{\nabla} \cdot \vec{m} - (\vec{m} \cdot \vec{\nabla})m_z] - K_u m_z^2 - \frac{M_s}{2} \mu_0 \vec{m} \cdot \vec{H}_d - M_s \vec{m} \cdot \vec{B}, \quad (1)$$

Parameter	PtCoPt ¹²	PtCoMgO ⁷	IrCoPt ⁴	PtCoNiCo ²⁵
Saturation magnetization M_s (10^3 A/m)	580	1400	956	600
Exchange constant A (10^{-12} J/m)	15	27.5	10	20
Perpendicular anisotropy constant K_u (10^6 J/m ³)	0.7	1.45	0.717	0.6
DMI parameter D (10^{-3} J/m ²)	3	2.05	1.6	3

Table 1. Micromagnetic parameters used in the simulations.

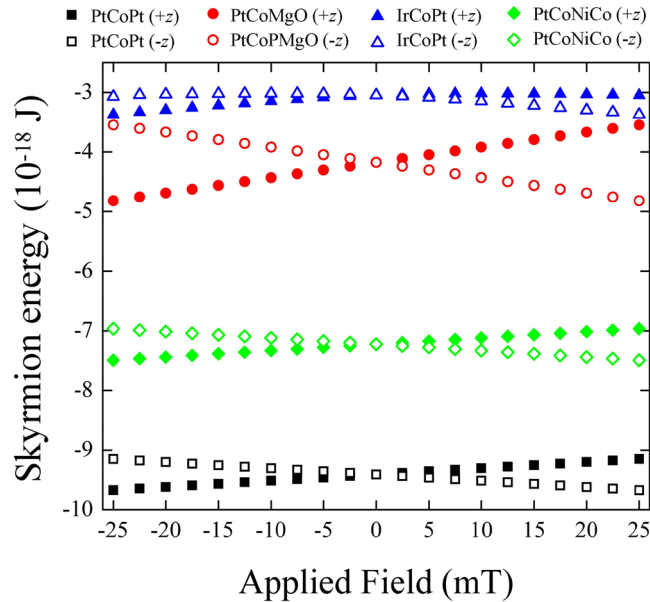


Figure 2. Numerical results obtained for the skyrmion energy as a function of the out-of-plane magnetic field for different materials and orientations of the skyrmion core with respect to the field. The dot diameter is 200 nm. Filled symbols stand for skyrmions with a core parallel to the field direction (z-axis) while the open symbols indicate skyrmions with the opposite core direction.

where the first term corresponds to the exchange energy with the stiffness constant A , the second term stands for the interface DMI with the constant D , the other terms correspond to the out-of-plane uniaxial magnetic anisotropy (where K_u is the uniaxial anisotropy constant), the magnetostatic and the Zeeman energies, respectively. The dot micromagnetic parameters are summarised in Table 1. The material quality factor $Q = 2K_u/\mu_0 M_s^2 > 1$ for each set of the parameters and D is large enough to ensure the Néel skyrmion metastability/stability in the zero out-of-plane magnetic field.

For the micromagnetic simulations we used the object-oriented micromagnetic framework (OOMMF) code with the extension accounting for the interfacial DMI²². The dot volume was discretized in cubic cells with the cell sizes of $0.5 \times 0.5 \times 0.6$ nm³. The out-of-plane magnetic field was varied in the interval from -20 mT to 30 mT.

To better understand the dependence of skyrmion diameter as a function of magnetic field we also used a semi-analytical approach. For this we defined the reduced magnetization vector \vec{m} of the skyrmion via the spherical angles (Θ, Φ) assuming that the z-axis is perpendicular to the dot plane (see Fig. 1) and there is no dependence of the magnetization on the thickness z -coordinate. The polar angle $\Theta = \Theta_0(\rho)$ is assumed to be a circularly symmetric function of the polar coordinate $\vec{p} = (\rho, \phi)$ and the azimuthal angle is $\Phi = \Phi_0 + \phi$, where $\Phi_0 = 0, \pi$ for the case of the Néel (hedgehog) skyrmion. For the description of the skyrmion magnetization configuration we used the following trial function

$$\tan \frac{\Theta_0(r)}{2} = \frac{r_s}{r} e^{\xi(r_s-r)}, \quad (2)$$

where $r_s = R_s/l_{ex}$ is the reduced skyrmion radius (expressed through the exchange length $l_{ex} = \sqrt{2A/\mu_0 M_s^2}$), $r = \rho/l_{ex}$, and $\xi^2 = Q - 1$. The trial function given in Eq. (2) was suggested by DeBonte²⁶ and previously used in ref.²⁷ to describe the axially symmetric magnetic solitons in a 2D Heisenberg easy axis ferromagnet showing a good agreement with the direct energy minimization method. More recently it was also successfully used to calculate the skyrmion stability diagram at zero field and the dependence of the skyrmion radius on the DMI strength and temperature²⁸ also showing a good agreement with micromagnetic modelling. For the isotropic case ($\xi = 0$) Eq. (2) recovers the well-known Belavin-Polyakov solution and leads to the finite exchange energy at $r \rightarrow 0$.

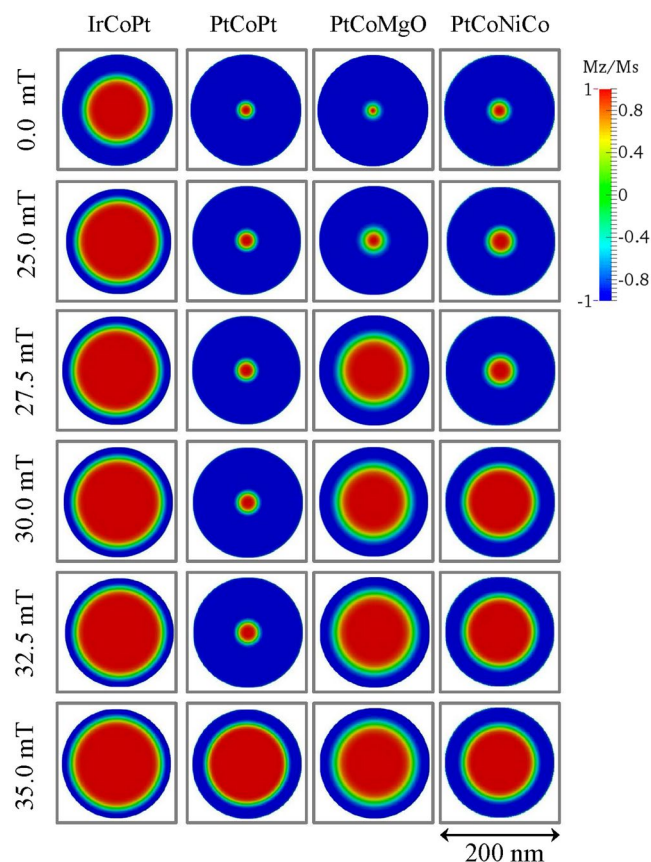


Figure 3. Snapshots of the Néel skyrmion magnetization configurations in a cylindrical dot of 200 nm diameter showing two types of skyrmions, a small one and a large one, stabilized by the dot border. Note that the initial configurations in all cases correspond to that of the skyrmion at zero out-of-plane magnetic field.

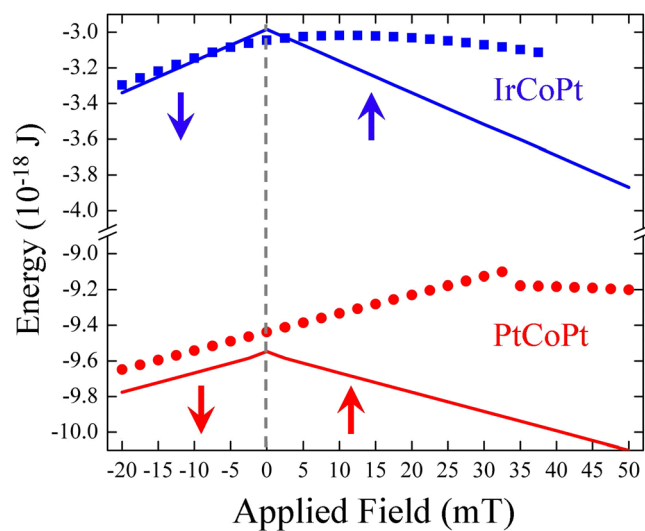


Figure 4. Comparison of the energies between a ferromagnetic state and a skyrmion state for the ultrathin nanodot of 200 nm in diameter made of IrCoPt (upper curves) and PtCoPt (lower curves) materials. The symbols correspond to the skyrmion state, while the solid lines correspond to the ferromagnetic state, which has magnetisation always parallel to the out-plane magnetic field.

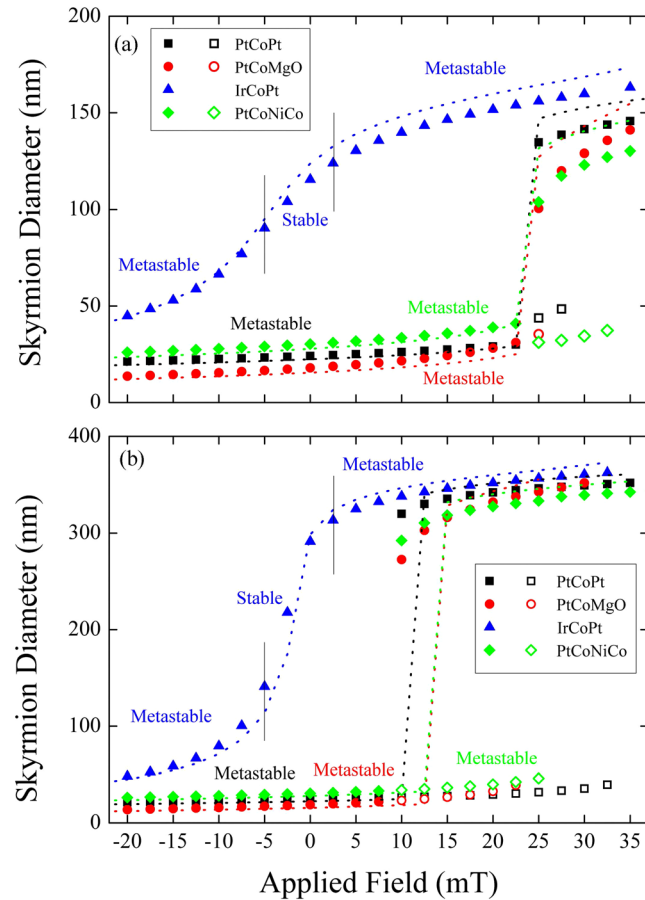


Figure 5. Dependence of the skyrmion diameter on the applied out-of-plane magnetic field for a ultrathin cylindrical dot of diameter (a) $d = 200$ nm and (b) $d = 400$ nm. Open symbols represent small radius skyrmion states with higher energy than the skyrmion states of larger diameter in the region of bi-stability. The dotted lines stand for the analytical calculations using the skyrmion profile given by Eq. (2). Here we plot the skyrmion sizes only for the skyrmion states of smaller energy.

The equilibrium skyrmion size is found by minimizing the energy functional $E = \int dV \varepsilon(\vec{m})$, using the energy density $\varepsilon(\vec{m})$ given in Eq. (1)

$$\frac{\partial E}{\partial r_s} = 0, \quad \frac{\partial^2 E}{\partial r_s^2} > 0 \quad (3)$$

Results and Discussion

Micromagnetic simulations. Figure 2 shows the comparison between the magnetic energies of the skyrmions with the core parallel and antiparallel to the bias field directions. The results indicate that skyrmion with the core antiparallel to the field direction always has lower energy than skyrmion with the core parallel to the field²⁹. In any case, the results are symmetric with respect to the field inversion so that we can restrict ourselves to positive fields only. However, we should remember that in our convention for the positive field there is always a skyrmion with a lower energy which can be obtained by symmetry from the results for negative fields.

Figure 3 illustrates the snapshots for the Néel skyrmion magnetization distribution in different materials for the circular dots with diameter $d = 200$ nm at different applied field values. Two distinct situations can be observed when the value of the magnetic field increases. For IrCoPt, the skyrmion is large and occupies almost the whole dot. In all other cases, the skyrmion is small for certain magnetic field values, but at some magnetic field it drastically increases its size until it becomes also large.

To tackle the difference between these situations we present below in Fig. 4 the comparison between the energies of the skyrmion state and the perpendicularly magnetized state applying the out-of-plane magnetic field in the positive (parallel to the skyrmion core) and negative (antiparallel to the skyrmion core) directions. For simplicity we present here the skyrmion with the core parallel to the z -axis. The other skyrmion energies can be easily seen by using the symmetry with negative fields. Also for the perpendicularly magnetized case (quasi-uniform state) we only indicate that of the smallest energy, i.e., parallel to the field.

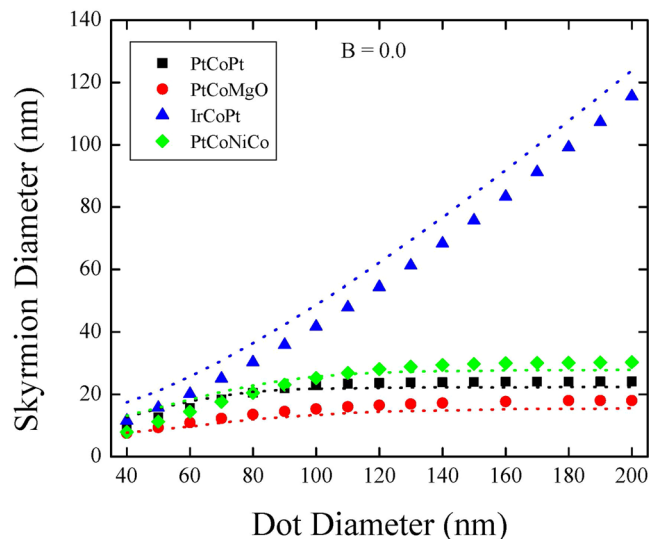


Figure 6. Simulated dependencies of the skyrmion diameter on the nanodot diameter for different materials and applied magnetic field $B = 0$. The dotted lines represent theoretical predictions.

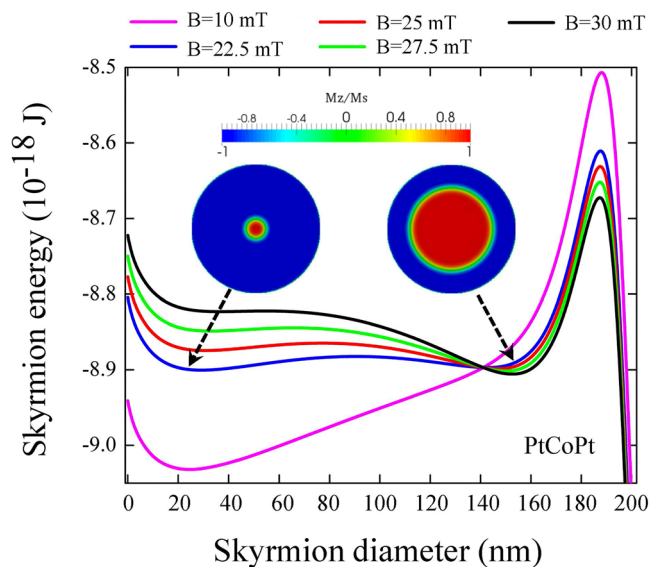


Figure 7. Skyrmion energy in PtCoPt dot of 200 nm in diameter, as function of the skyrmion diameter for different values of the out-of-plane magnetic field near the critical value calculated by analytical approach.

The important conclusion of the energy considerations is that in the case of IrCoPt the skyrmion is a ground state of the dot at zero field and there exists a region of its stability in some field interval around. In all other considered cases such as PtCoPt presented in Fig. 4 the skyrmion is metastable. Note that only for one of the four considered material parameter sets the skyrmion is the system ground state. This is in agreement with our recent micromagnetic simulations showing that the stable skyrmions are very rare (Aranda, A.R., *et al.*, Submitted, 2018) and most of the skyrmions reported in the literature are metastable.

Our main results are presented in Fig. 5, where we show the dependence of skyrmion radii on the applied field values for the dots with two diameters $d = 200$ nm and $d = 400$ nm and four chosen sets of the material parameters (see Table 1). Note the existence of two distinct characteristic dependencies. In the case of IrCoPt, the skyrmion is stable at zero field. Its diameter is large at zero field and strongly increases when the field increases from zero until the skyrmion becomes metastable and the field dependence of the skyrmion radius becomes weak.

In the other cases, the skyrmion is always metastable and field dependence of its size at low fields is weak until some critical field value is reached, where a sudden increase of the skyrmion diameter takes place. Around this field there are two types of the metastable skyrmions: a small and a large one and the field dependence of the skyrmion radius is characterized by a hysteretic behavior as a function of the applied field. In this region the skyrmion of the larger diameter (i.e., stabilized by the dot boarder) has a smaller energy than the small radius

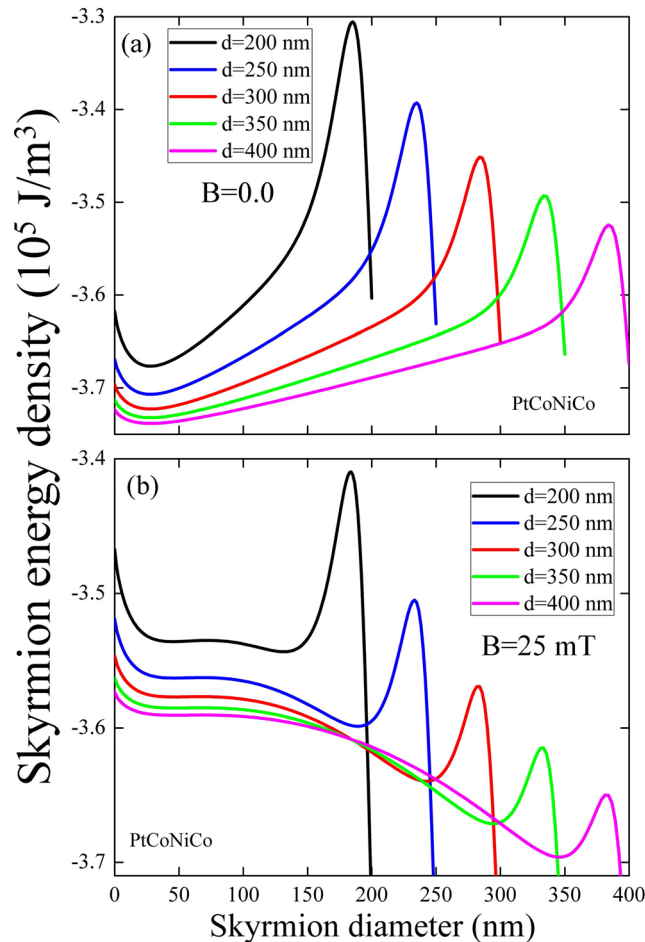


Figure 8. Skyrmion energy density as a function of the skyrmion diameter in a dot of PtCoNiCo for different values of the dot diameter, calculated by analytical approach for the out-of-plane magnetic field (a) $B = 0$ and (b) $B = 25$ mT.

skyrmion. Note that the critical magnetic field for the transition between small and large size skyrmion is larger in the smaller dots. The hysteresis width is larger in larger dots.

Figure 6 presents the skyrmion diameter as a function of the dot diameter at zero out-of-plane field. In very small dots all skyrmions have similar dimensions stabilized by the dot boarder. While the small metastable skyrmions reveal a weak increase of their diameter with the diameter of the dot, the large stable skyrmions reveal a strong dependence keeping the ratio between the diameter of the skyrmion and the dot approximately as constant.

Analytical calculations. The results of the analytical model are presented by the dotted lines in Figs 5 and 6 as a function of the out-of-plane field and as a function of the dot diameter, respectively. For simplicity the lines indicate the skyrmion of the lowest energy only. Given the approximate ansatz for the skyrmion profile, Eq. (2), we consider that the agreement between theoretical and direct modelling calculations is excellent. Particularly, the analytical model reproduce well the bi-stability of the skyrmion state at high fields.

In Fig. 7 we present the analytical skyrmion energy as a function of its diameter for PtCoPt dot near the critical field. The graph clearly demonstrates how an additional minimum corresponding to the large skyrmion diameter appears near the dot edge, with the energy smaller than that for the skyrmion of the small diameter. The small size Néel skyrmion becomes unstable at high values of the out-of-plane field. Note that a similar behavior was reported recently in ref.²⁸ as a function of temperature. The skyrmion bi-stability at zero applied field was simulated recently in thick multilayer dots due to the effect of the dipolar interactions³⁰. Importantly, our model also allows us to estimate the energy barrier between the states with the skyrmions of two diameters. They appears to be small, of the order of several $k_B T$ at room temperature meaning that at some values of the out-of-plane field the skyrmion will superparamagnetically fluctuate from one diameter to another. The shallow minima of the skyrmion energy vs. the skyrmion radius result in the low frequency breathing modes³¹. The breathing mode frequency then is in sub-GHz range and can be close to the frequency of the lowest skyrmion gyrotropic mode related to its topological charge³². When the out-of-plane magnetic field increases the skyrmion with large diameter become more and more stable against thermal fluctuations.

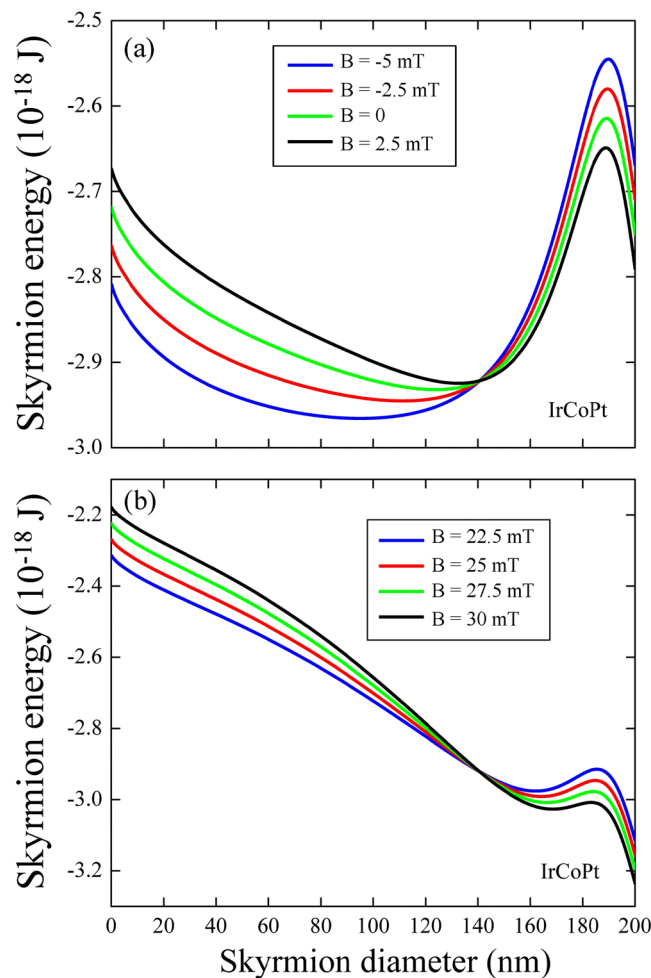


Figure 9. Skyrmion energy in a IrCoPt dot of 200 nm in diameter, as function of the skyrmion diameter for different values of the out-of-plane magnetic field (a) in the stable region (b) in the metastable region.

At the same time, the energy barriers between the small diameter skyrmion and the perpendicular saturated states (of the order of $30\text{--}40 k_B T$) are large enough to provide the skyrmion thermal stability.

Another illustration is presented in Fig. 8 for PtCoNiCo material and varying the dot diameter. We clearly observe that at zero field (Fig. 8(a)) the energy minimum is located near the small values of the skyrmion diameter and is only weakly displaced to the right for larger dot diameters. At the same time, at $B = 25$ mT (Fig. 8(b)) there are two energy minima: one is located at a small skyrmion diameter value and the other one is located at large diameter value, stabilized by the dot boarder and with smaller magnetic energy. The minimum corresponding to the small skyrmion diameter is shallow and disappears increasing the bias field strength. Whereas, the minimum corresponding to the large skyrmion diameter becomes deeper. In the other words, the small radius metastable skyrmion does not feel the dot boundary. The large size skyrmion feels well the dot boundary and the skyrmion edge stops at the distance approximately of 50 nm from it.

In the case of IrCoPt shown in Fig. 9(a) in the skyrmion stability region, e.g., at zero out-of-plane magnetic field, the energy minimum is localized at large values of the skyrmion diameters and is strongly displaced with a relatively small change in the bias field. In the metastability region as in the example presented in Fig. 9(b) this minimum is always localized near the dot edge and only weakly displaces to higher skyrmion diameter values with the field increase.

Conclusions

Micromagnetic simulations and analytical calculations were performed to study the size of the Néel skyrmion confined in a cylindrical ultrathin nanodot. The results show a very good agreement between both methods allowing us to conclude about good accuracy of the ansatz given in Eq. (2) for the Néel skyrmion profile.

There are two different types of skyrmions (large and small size) with distinct dependence of their radius on the applied out-of-plane field. The large radius skyrmions are rare, stable at zero field and possess strong and continuous dependence of their radius on the applied out-of-plane field and dot size. These skyrmions undergo the transition between stable and metastable states. In the metastable state their size dependence on the applied field becomes weak.

In the other more frequent case, the skyrmions have small radius at zero field and are always metastable. They are characterized by a weak dependence of their radius on the applied field until some critical field is reached at which the radius increases suddenly. The skyrmion energy is bi-stable close to this critical field and there is co-existence of a small and a large size metastable skyrmions within some field interval.

Therefore, we calculated a universal behavior of the Néel skyrmions in ultrathin dots with interface induced DMI. This opens a possibility to detect experimentally the skyrmion metastability/stability just looking at the skyrmion radius variation as a function of the applied out-of-plane magnetic field. We also calculated that the hysteresis process is a property of metastable skyrmions only. In this case, three skyrmion states (all metastable) may co-exist: two states with the skyrmion cores are parallel to the field and one - antiparallel to it.

References

- Fert, A., Cros, V. & Sampaio, J. Skyrmions on the track. *Nat. Nanotechnol.* **8**, 152 (2013).
- Nagaosa, N. & Tokura, Y. Topological properties and dynamics of magnetic skyrmions. *Nat. Nanotechnol.* **8**, 899 (2013).
- Fert, A., Reyren, N. & Cros, V. Magnetic skyrmions: advances in physics and potential applications. *Nature Rev. Mat.* **2**, 17031 (2017).
- Moreau-Luchaire, C. *et al.* Additive interfacial chiral interaction in multilayers for stabilization of small individual skyrmions at room temperature. *Nat. Nanotechnol.* **11**, 444 (2016).
- Yang, H., Thiaville, A., Rohart, S., Fert, A. & Chshiev, M. Anatomy of Dzyaloshinskii-Moriya Interaction at Interfaces. *Phys. Rev. Lett* **115**, 267210 (2015).
- Woo, S. *et al.* Observation of room-temperature magnetic skyrmions and their current-driven dynamics in ultrathin metallic ferromagnets. *Nat. Mater.* **15**, 501 (2016).
- Boulle, O. *et al.* Room-temperature chiral magnetic skyrmions in ultrathin magnetic nanostructures. *Nat. Nanotechnol.* **11**, 449–454 (2016).
- Kézsmárki, I. *et al.* Néel-type skyrmion lattice with confined orientation in the polar magnetic semiconductor GaV_4S_8 . *Nat. Mater.* **14**, 1116 (2015).
- Tomasello, R. *et al.* A strategy for the design of skyrmion racetrack memories. *Sci. Rep.* **4**, 6784 (2014).
- Rohart, S., Miltat, J. & Thiaville, A. Path to collapse for an isolated Néel skyrmion. *Phys. Rev. B* **93**, 214412 (2016).
- Bessarab, P. F. Comment on “Path to collapse for an isolated Néel skyrmion”. *Phys. Rev. B* **95**, 136401 (2017).
- Sampaio, J., Cros, V., Rohart, S., Thiaville, A. & Fert, A. Nucleation, stability and current-induced motion of isolated magnetic skyrmions in nanostructures. *Nat. Nanotechnol.* **8**, 839–844 (2013).
- Jiang, W. *et al.* Direct observation of the skyrmion Hall effect. *Nat. Phys.* **13**, 162 (2016).
- Litzius, K. *et al.* Skyrmion Hall effect revealed by direct time-resolved X-ray microscopy. *Nat. Phys.* **13**, 170 (2017).
- Yu, X. *et al.* Skyrmion flow near room temperature in an ultralow current density. *Nat. Commun.* **3**, 988 (2012).
- Zhou, Y. *et al.* Dynamically stabilized magnetic skyrmions. *Nat. Commun.* **6**, 8193 (2015).
- Vidal-Silva, N., Riveros, A. & Escrig, J. J. Stability of Neel skyrmions in ultra-thin nanodots considering Dzyaloshinskii-Moriya and dipolar interactions. *J. Magn. Magn. Mater.* **443**, 116–123 (2017).
- Novak, R. L., Garcia, F., Novais, E. R. P., Sinnecker, J. P. & Guimaraes, A. P. Micromagnetic study of skyrmion stability in confined magnetic structures with perpendicular anisotropy, arXiv:1709.07559v1.
- Guslienko, K. Y. Skyrmion State Stability in Magnetic Nanodots With Perpendicular Anisotropy. *IEEE Magn. Lett.* **6**, 4000104 (2015).
- Rowland, J., Banerjee, S. & Randeria, M. Skyrmions in chiral magnets with Rashba and Dresselhaus spin-orbit coupling. *Phys. Rev. B* **93**, 020404(R) (2016).
- Banerjee, S., Rowland, J., Erten, O. & Randeria, M. Enhanced Stability of Skyrmions in Two-Dimensional Chiral Magnets with Rashba Spin-Orbit Coupling. *Phys. Rev. X* **4**, 031045 (2014).
- Rohart, S. & Thiaville, A. Skyrmion confinement in ultrathin film nanostructures in the presence of Dzyaloshinskii-Moriya interaction. *Phys. Rev. B* **88**, 184422 (2013).
- Beg, M. *et al.* Ground state search, hysteretic behaviour, and reversal mechanism of skyrmionic textures in confined helimagnetic nanostructures. *Sci. Rep.* **5**, 17137 (2015).
- Kim, J.-V. *et al.* Breathing modes of confined skyrmions in ultrathin magnetic dots. *Phys. Rev. B* **90**, 064410 (2014).
- Ryu, K. S., Yang, S.-H., Thomas, L. & Parkin, S. S. P. Chiral spin torque arising from proximity-induced magnetization. *Nat. Commun.* **5**, 3910 (2014).
- DeBonte, W. J. Properties of thick-walled cylindrical magnetic domains in uniaxial platelets. *J. Appl. Phys.* **44**, 1793 (1973).
- Sheka, D. D., Ivanov, B. A. & Mertens, F. G. Internal modes and magnon scattering on topological solitons in two-dimensional easy-axis ferromagnets. *Phys. Rev. B* **64**, 024432 (2001).
- Tomasello, R. *et al.* Origin of temperature and field dependence of magnetic skyrmion size in ultrathin nanodots. *Phys. Rev. B* **97**, 060402 (2018).
- Riveros, A., Vidal-Silva, N., Tejo, F. & Escrig, J. Analytical and numerical Ku B phase diagrams for cobalt nanostructures: stability region for a Bloch skyrmion. *J. Magn. Magn. Mater.* arXiv:1706.08876v2 (In Press, 2017).
- Zelent, M., Tobik, J., Krawczyk, M., Guslienko, K. Y. & Mruczkiewicz, M. Bi-Stability of Magnetic Skyrmions in Ultrathin Multilayer Nanodots Induced by Magnetostatic Interaction. *Phys. Status Solidi (RRL) - Rapid Res. Lett.* **11**, 1700259 (2017).
- Mruczkiewicz, M. *et al.* Spin excitation spectrum in a magnetic nanodot with continuous transitions between the vortex, Bloch-type skyrmion, and Néel-type skyrmion states. *Phys. Rev. B* **95**, 094414 (2017).
- Guslienko, K. Y. & Gareeva, Z. V. Gyrotropic Skyrmion Modes in Ultrathin Magnetic Circular Dots. *IEEE Magn. Lett.* **8**, 4100305 (2017).

Acknowledgements

F.T., A.R., and J.E. acknowledge financial support from the Fondecyt Grant No. 1150952, Fondecyt Grant 3180470 and DICYT Grant 041731EM-POSTDOC from VRIDEI-USACH, and Financiamiento Basal para Centros Científicos y Tecnológicos de Excelencia FB0807. CONICYT Ph.D. Program Fellowships is also acknowledged. K.G. acknowledges support by IKERBASQUE (the Basque Foundation for Science) and the European Union Horizon 2020 Research and Innovation Programme under Marie Skłodowska-Curie Grant Agreement No. 644348. The work of K.G. and O.C.-F. was supported by the Spanish Ministry of Economy and competitiveness under the project FIS2016-78591-C3-3-R.

Author Contributions

The problem was designed and proposed by F. Tejo and O. Chubykalo-Fesenko. The micromagnetic simulations were developed by F. Tejo. The theoretical model was proposed by K.Y. Guslienko. A. Riveros and J. Escrig obtained analytical results. All the authors analysed the results. The article was written by O. Chubykalo-Fesenko. Finally, the article was reviewed by all authors.

Additional Information

Competing Interests: The authors declare no competing interests.

Publisher's note: Springer Nature remains neutral with regard to jurisdictional claims in published maps and institutional affiliations.



Open Access This article is licensed under a Creative Commons Attribution 4.0 International License, which permits use, sharing, adaptation, distribution and reproduction in any medium or format, as long as you give appropriate credit to the original author(s) and the source, provide a link to the Creative Commons license, and indicate if changes were made. The images or other third party material in this article are included in the article's Creative Commons license, unless indicated otherwise in a credit line to the material. If material is not included in the article's Creative Commons license and your intended use is not permitted by statutory regulation or exceeds the permitted use, you will need to obtain permission directly from the copyright holder. To view a copy of this license, visit <http://creativecommons.org/licenses/by/4.0/>.

© The Author(s) 2018